

Prevascularization of a Gas-Foaming Macroporous Calcium Phosphate Cement Scaffold Via Coculture of Human Umbilical Vein Endothelial Cells and Osteoblasts

WahWah Thein-Han, MD, PhD,¹ and Hockin H.K. Xu, PhD¹⁻⁴

The lack of a vasculature in tissue-engineered constructs is currently a major challenge in tissue regeneration. There has been no report of prevascularization of macroporous calcium phosphate cement (CPC) via coculture of endothelial cells and osteoblasts. The objectives of this study were to (1) investigate coculture of human umbilical vein endothelial cells (HUVEC) and human osteoblasts (HOB) on macroporous CPC for the first time; and (2) develop a new microvasculature-CPC construct with angiogenic and osteogenic potential. A gas-foaming method was used to create macropores in CPC. HUVEC and HOB were seeded with a ratio of HUVEC:HOB=4:1, at 1.5×10^5 cells/scaffold. The constructs were cultured for up to 42 days. CPC with a porosity of 83% had a flexural strength (mean \pm SD; $n=6$) of 2.6 ± 0.2 MPa, and an elastic modulus of 340 ± 30 MPa, approaching the reported values for cancellous bone. Reverse transcription-polymerase chain reaction showed that HUVEC+HOB coculture on CPC had much higher vascular endothelial growth factor (VEGF) and collagen I expressions than monoculture ($p < 0.05$). Osteogenic markers alkaline phosphatase, osteocalcin (OC), and runt-related transcription factor 2 (*Runx2*) were also highly elevated. Immunostaining of PECAM1 (CD31) showed abundant microcapillary-like structures on CPC in coculture at 42 days, as HUVEC self-assembled into extensive branches and net-like structures. However, no microcapillary was found on CPC in monoculture. In immunohistochemical staining, the neo-vessels were strongly positive for PECAM1, the von Willebrand factor, and collagen I. Scanning electron microscopy revealed microcapillary-like structures mingling with mineral nodules on CPC. Cell-synthesized minerals increased by an order of magnitude from 4 to 42 days. In conclusion, gas-foaming macroporous CPC was fabricated and HUVEC+HOB coculture was performed for prevascularization, yielding microcapillary-like structures on CPC for the first time. The novel macroporous CPC-microvasculature construct is promising for a wide range of orthopedic applications with enhanced angiogenic and osteogenic capabilities.

Introduction

BONE DEFECTS AND nonunions are a growing problem worldwide. Seven million people suffer bone fractures each year in the United States.¹ Health care costs plus the lost wages for people with musculoskeletal diseases reached ~\$849 billion in 2004 in the United States, or 7.7% of the national gross domestic product.² These numbers are predicted to increase due to an aging population, as the need for bone repair increases with the baby-boomers entering into retirement and having longer life expectancies.³⁻⁷ Recent studies on tissue engineering have demonstrated exciting

potential to meet this need.⁸⁻¹⁰ Stem cells were guided for osteogenic differentiation and combined with tissue-engineered scaffolds for bone regeneration.^{6,11-15}

However, a major limitation of bone tissue engineering is the difficulty to vascularize the construct.¹⁶⁻¹⁸ When a scaffold is seeded with cells and implanted *in vivo*, only the cells within the proximity of 100–200 μ m from a capillary can obtain an adequate supply of oxygen and nutrients to survive.^{16,17} Insufficient vascularization will cause nutrient deficiencies and hypoxia of the seeded cells, resulting in decreased tissue function and cell death at the core. An important method to overcome this problem is *in vitro*

¹Biomaterials & Tissue Engineering Division, Department of Endodontics, Prosthodontics and Operative Dentistry, University of Maryland Dental School, Baltimore, Maryland.

²Center for Stem Cell Biology & Regenerative Medicine, University of Maryland School of Medicine, Baltimore, Maryland.

³University of Maryland Marlene and Stewart Greenebaum Cancer Center, University of Maryland School of Medicine, Baltimore, Maryland.

⁴Department of Mechanical Engineering, University of Maryland, Baltimore, Maryland.

prevascularization.^{16,17} Several studies investigated the coculture of endothelial cells and osteoprogenitor cells to form a prevascular network *in vitro* for bone tissue engineering.^{19–21} A coculture system using endothelial cells and osteoblasts was investigated on scaffolds, including porous hydroxyapatite, porous β -tricalcium phosphate, porous nickel-titanium, and silk fibroin nets.²⁰ This method produced a tissue-like self-assembly of cells, with endothelial cells forming microcapillary-like structures.²⁰ A starch-based scaffold was also used for the coculture approach where osteoblasts and endothelial cells were simultaneously cultured, yielding microcapillary-like structures.²¹ These studies demonstrated the benefits of the *in vitro* prevascularization method in developing the vascularization needed for bone tissue-engineering applications.

Due to their excellent biocompatibility and chemical similarity to the minerals in natural bones, calcium phosphate (CaP) biomaterials are important for hard tissue repair.^{11,22–28} CaP implants possess osteoconductivity and bioactivity, which can facilitate the formation of a functional interface with a neighboring bone.^{5,11,29,30} Calcium phosphate cement (CPC) can be molded and set *in situ* to form a scaffold that can be resorbed and replaced by new bone, and can be injected to fill complex-shaped bone defects.^{23–25,29} The first CPC was developed in 1986 and approved in 1996 by the Food and Drug Administration (FDA) for repairing craniofacial defects.^{23,31} Various new CPC compositions have been developed.^{12,24,25,32–34} Other studies have incorporated degradable fibers, chitosan, and porogen to develop injectable, load-bearing, and macroporous CPC scaffolds.^{35–37} Recent studies have investigated injectable CPC scaffold encapsulating stem cells for bone tissue engineering.^{15,38} However, to date, there has been no report on *in vitro* prevascularization of CPC via coculture of endothelial cells and osteoblasts.

Therefore, the objectives of the present study were to (1) investigate the coculture of human umbilical vein endothelial cells (HUVEC) and human osteoblasts (HOB) on the macroporous CPC scaffold for the first time; (2) develop a novel microvasculature-CPC construct; and (3) investigate the angiogenic and osteogenic effects of the HUVEC-HOB-CPC scaffold. It was hypothesized that (1) The coculture of HUVEC and HOB on macroporous CPC will greatly enhance the formation of a microcapillary network, compared to HUVEC monoculture on CPC; (2) A neovascularized bone construct with matrix mineralization can be formed via HUVEC and HOB coculture on macroporous CPC *in vitro*.

Materials and Methods

Fabrication of gas-foaming macroporous CPC scaffold

Tetracalcium phosphate (TTCP: $\text{Ca}_4[\text{PO}_4]_2\text{O}$) was synthesized using equimolar amounts of dicalcium phosphate anhydrous (DCPA: CaHPO_4) and calcium carbonate (J.T. Baker). The reactant was ground to obtain TTCP particles of 1 to 80 μm , with a median of 17 μm .^{26,36} DCPA was ground to obtain a median particle size of 1 μm . TTCP and DCPA powders were mixed at a molar ratio of 1:1 to form the CPC powder.^{26,36} Chitosan lactate (VANSON) was dissolved in water at a chitosan/(chitosan+water) mass fraction of 15% to form the liquid.²⁶ CPC powder:liquid mass ratio was 2:1. A gas-foaming method was used to create macropores in CPC.^{15,39} Briefly, citric acid (citric acid monohydrate,

$\text{C}_6\text{H}_8\text{O}_7\cdot\text{H}_2\text{O}$) and sodium hydrogen carbonate (NaHCO_3) (Sigma) were used as porogen in CPC. The acid-base reaction of citric acid with NaHCO_3 produced CO_2 bubbles in CPC, resulting in macropores in the set CPC.^{15,39} NaHCO_3 was added to the CPC powder, at a $\text{NaHCO}_3/(\text{NaHCO}_3 + \text{CPC powder})$ mass fraction of 20%, following a previous study.¹⁵ $\text{C}_6\text{H}_8\text{O}_7\cdot\text{H}_2\text{O}$ was added to the CPC liquid, to maintain a fixed $\text{NaHCO}_3/(\text{NaHCO}_3 + \text{C}_6\text{H}_8\text{O}_7\cdot\text{H}_2\text{O})$ mass fraction of 54.52%.³⁹ For mechanical reinforcement, a resorbable suture fiber (Vicryl, polyglactin 910; Ethicon) was cut to filaments of a length of 3 mm and mixed with CPC paste at a fiber volume fraction of 20%.¹⁵ These fiber length and volume fraction values were previously shown to yield a CPC paste that was fully injectable.³⁸ Details of the processing, microstructure, and physical properties of the gas-foaming CPC were reported elsewhere.³⁹

Mechanical property and porosity of the scaffolds

The CPC composite paste was placed into a mold of $3 \times 4 \times 25$ mm. The specimens were incubated at 37°C for 4 h for the CPC to set, and then demolded and immersed in water at 37°C for 20 h. The specimens were then fractured in three-point flexure with a span of 20 mm at a crosshead speed of 1 mm/min on a Universal Testing Machine (5500R; MTS). The flexural strength and elastic modulus were measured.

The CPC porosity was measured by using a porosimeter (PoreMaster 33; Quantachrome Instruments). The specimens were dried in a vacuum oven at 60°C for 24 h, and then placed in a mercury intrusion chamber of the porosimeter.⁴⁰ The chamber was evacuated and gradually filled with mercury up to a pressure of 30,000 psi. Plots of intruded volume versus pressure were recorded. The known chamber volume and mercury density enabled the specimen's porosity to be calculated.⁴⁰

HUVEC-HOB coculture on macroporous CPC scaffolds

HUVEC (Lonza) were cultured in the endothelial cell basal medium-2 (EBM-2, Lonza) supplemented with 100 U/mL penicillin and 100 $\mu\text{g}/\text{mL}$ streptomycin sulfate in a humidified incubator (5% CO_2 , 37°C). HOB (Lonza) were cultured in the osteoblast basal medium supplemented with 100 U/mL penicillin and 100 $\mu\text{g}/\text{mL}$ streptomycin sulfate. Passage 4 cells were used. Cells at 80% confluence were trypsinized and washed with PBS.

Macroporous CPC disks of 12 mm in diameter and 1.5 mm in thickness were fabricated. The scaffolds were preincubated with a culture medium for 3 h. Then, they were placed individually in 24-well plates. For coculture, the mixed HUVEC-HOB suspension (at a ratio of HUVEC:HOB=4:1) was seeded dropwise on the top of the CPC scaffold at 1.5×10^5 cells/scaffold.²¹ For the monoculture control, HUVEC were seeded on CPC at 1.5×10^5 cells/scaffold. The constructs were cultured in the EBM in a humidified incubator (5% CO_2 , 37°C) for 42 days.²⁰ The EBM was replaced every 2 days.

Angiogenic and osteogenic gene expressions

Quantitative real-time reverse transcription-polymerase chain reaction measurement (qRT-PCR, 7900HT; Applied Biosystems) was performed for cell-CPC constructs. The

assessments were performed at 1, 14, and 21 days, the time range within which the vascular endothelial growth factor (VEGF)²¹ and osteogenic gene expression peaks¹⁵ were previously observed. The total cellular RNA from CPC samples were extracted with the TRIzol reagent (Invitrogen). The RNA concentration was measured via NanoDrop (Bio-Rad). RNA was reverse transcribed into cDNA (High-Capacity cDNA transcription kit, TaqMan). TaqMan gene expression kits were used to measure the transcript levels of the following genes: *VEGF A* (HS00900055_ml), alkaline phosphatase (*ALP*) (Hs00758162_m1), collagen type I (*Col I*) (Hs00164004), and runt-related transcription factor2 (*Runx2*) (Hs00231692_m1).^{21,41} The relative expression for each target gene was evaluated using the $2^{-\Delta\Delta C_t}$ method.⁴² The C_t values of target genes were normalized by the C_t of the human housekeeping gene, glyceraldehyde 3-phosphate dehydrogenase (*GAPDH*) (Hs99999905) to obtain the ΔC_t values.^{38,43}

Immunostaining of PECAM1 (CD31)

The microvascular structure formation by endothelial cells and their organization on CPC scaffolds were investigated via endothelial cell-specific PECAM1 staining.^{20,21} The cell-scaffold constructs up to 42 days were stained with PECAM1 (CD31) (Invitrogen). The samples were fixed with 4% paraformaldehyde for 20 min, permeabilized with 0.1% Triton X-100 for 5 min, and blocked with 0.1% bovine serum albumin for 30 min. Subsequently, the samples were immunostained with the primary mouse monoclonal antibody anti-human CD31 (1:50) at 4°C overnight, followed by the secondary antibody mouse anti-mouse Alexa Fluor 488 (green fluorescence) (Invitrogen). Cell nuclei were stained with DAPI (1:1000) (Sigma). The samples were mounted in the Fluor-mount aqueous medium (Sigma) and viewed under epifluorescence microscopy (TE2000S; Nikon) and confocal laser scanning microscopy (Zeiss LSM510 Meta). The capillaries were stained green and showed as tube-like structures. The length of capillaries was measured and added together to obtain the cumulative length of capillaries for each image using Image-Pro Plus software (Media Cybernetics). The cumulative length of capillaries of the image was then divided by the area of that image, to yield the cumulative vessel length per scaffold surface area.

Analysis of neovascular growth via immunohistochemical staining

Immunohistochemical staining was performed on thin sections to evaluate the neovascular formation.²¹ CPC constructs cocultured for 42 days were fixed with neutral-buffered formalin and cut to sections of a thickness of 150–200 μm (IsoMet). The CPC sections were immunostained using specific primary antibodies for the endothelial cell marker CD31 (mouse anti-human PECAM1, 1:50; Invitrogen), von Willebrand factor (vWF) (rabbit anti-human vWF, 1:100; Chemicon), collagen type I (mouse anti-human Col I, 1:100; Chemicon), and osteonectin (ON) (rabbit anti-human ON, 1:100; Chemicon). vWF is synthesized within endothelial cells, which line the inside surface of blood vessels. The samples were incubated in a blocking solution, followed by a biotinylated secondary antibody solution using Histostain Plus kits (Invitrogen) for immunohistochemical assay. Enhanced horseradish peroxidase-conjugated streptavidin was

bound to the secondary antibody. 3,3-Diaminobenzidine was used to create an intense brown/red deposit around the antigen/antibody/enzyme complex. The samples were counter stained with Mayer's hematoxylin (Sigma).

Scanning electron microscopy

CPC constructs cocultured for 42 days were examined using scanning electron microscopy (SEM, Quanta 200; FEI). The constructs were fixed with 2.5% glutaraldehyde in 0.1 M cacodylate buffer at pH 7.4, dehydrated with a graded series of ethanol (25%–100%), and rinsed with hexamethyldisilazane. The CPC surface was sputter coated with platinum.

Osteogenesis in coculture on CPC

Alizarin Red S (ARS) staining was used to examine bone mineralization via cells on CPC cocultured for 42 days. The constructs were washed with PBS, fixed with 10% formaldehyde, and stained with ARS (Millipore) for 20 min, which stained calcium-rich deposits by cells into a red color. An osteogenesis assay (Millipore) was used to extract the stained minerals and measure the ARS concentration at OD₄₀₅, following the manufacturer's instructions.⁴⁴ The ARS standard curve was done with a known concentration of the dye. Control CPC scaffolds with the same compositions and treatments, but without cell seeding, were also measured. The control's ARS concentration was subtracted from the ARS concentration of the cell-seeded scaffolds, to yield the net mineral concentration synthesized by the cells.⁴⁴

Statistical analysis

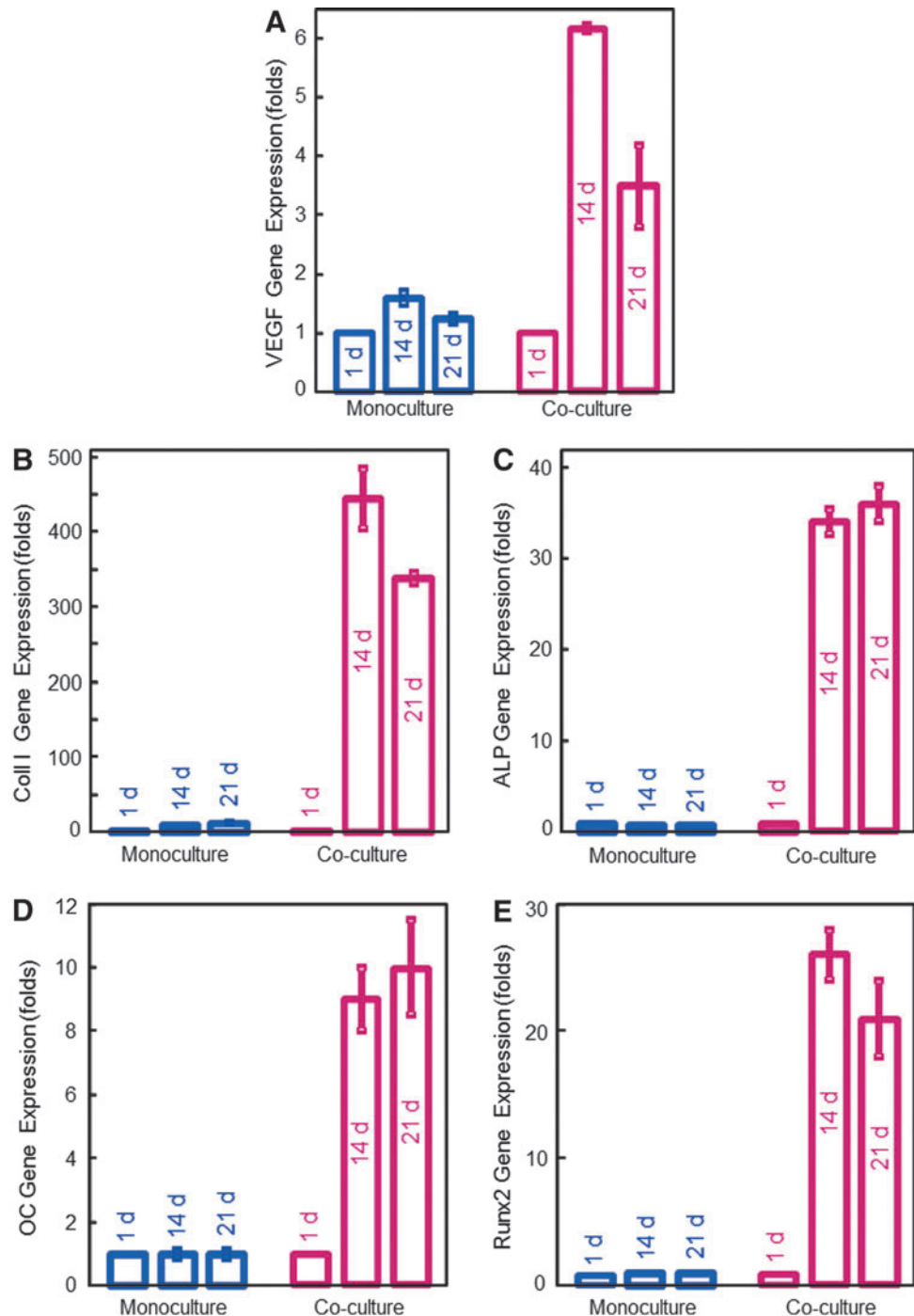
One-way and two-way ANOVA were performed to detect significant ($\alpha=0.05$) effects of the variables. Tukey's multiple comparison procedures were used to group and rank the measured values, and Dunn's multiple comparison tests were used on data with non-normal distribution or unequal variance, both at a family confidence coefficient of 0.95.

Results

The flexural strength of macroporous CPC was measured (mean \pm SD; $n=6$) to be 2.6 ± 0.2 MPa. The elastic modulus of the scaffold was 340 ± 30 MPa. The pore volume fraction of CPC was measured to be $83\% \pm 4\%$. CPC consisted of micropores with sizes of less than 1 μm to several μm , as well as macropores with sizes ranging from about 50 to 800 μm . The average macropore size was $\sim 490 \mu\text{m}$ as measured for 100 randomly selected macropores.

The RT-PCR results are plotted in Figure 1 (mean \pm SD; $n=6$). The genetic profiles confirmed that the HUVEC + HOB coculture had much higher angiogenic and osteogenic expressions compared to the HUVEC monoculture. In coculture, upregulated *VEGF* expression was four times higher than monoculture at 14 days. ECM-related cell structure collagen I expression in coculture at 14 days was 444 ± 41 , compared to 11.8 ± 0.4 for HUVEC monoculture. Osteogenic markers *ALP*, osteocalcin (*OC*), and runt-related transcription factor 2 (*Runx2*) also greatly increased with time. A highly upregulated *ALP* of (83 ± 5) folds was observed in coculture at 14 days, compared to an *ALP* of 1 at 1 day. *OC* and *Runx2* at 14 and 21 days in coculture were also highly elevated, compared to 1 day ($p < 0.05$).

FIG. 1. Angiogenic and osteogenic gene expressions measured via reverse transcription–polymerase chain reaction (mean \pm SD; $n=6$). In human umbilical vein endothelial cells and human osteoblast (HUVEC+HOB) coculture on macroporous calcium phosphate cement (CPC), (A) vascular endothelial growth factor (VEGF), (B) collagen I, (C) alkaline phosphatase (ALP), (D) osteocalcin (OC), and (E) runt-related transcription factor 2 (*Runx2*) gene expressions were all highly elevated at 14 and 21 days, compared to those at 1 day ($p<0.05$). In contrast, there was little up-regulation in monoculture. These results indicate that HUVEC+HOB coculture on CPC had successful angiogenic and osteogenic differentiation. Color images available online at www.liebertpub.com/tea



In Figure 2 with immunostaining of PECAM1, the organization of HUVEC on macroporous CPC exhibited microcapillary-like structures in coculture at 42 days. HUVEC self-assembled into abundant branches and net-like structures (Fig. 2A). At a higher magnification (Fig. 2B), the microcapillary-like structure (long arrows) was seen to extend throughout the HOB (blue nuclei, with no green stain) to form multiple sprouts. An example of a branching point for the highly branched structure is shown in Figure 2C. A higher magnification in Figure 2D showed that the diameter of the microcapillary-like structures was made up of 2–3 cells

as indicated by the location of nuclei (arrows) and the PECAM1 staining. These results indicate that the lumens were branched and the microcapillary-like structures on CPC were highly interconnected.

In contrast, microcapillary-like structures were not observed in HUVEC monoculture for up to 42 days on CPC (Fig. 3A). In monoculture of HUVEC, cells attached to macroporous CPC and proliferated and increased the coverage of the CPC surface. However, HUVEC distributed randomly as clumps or monolayers of cells, with no microcapillary-like structures on CPC.

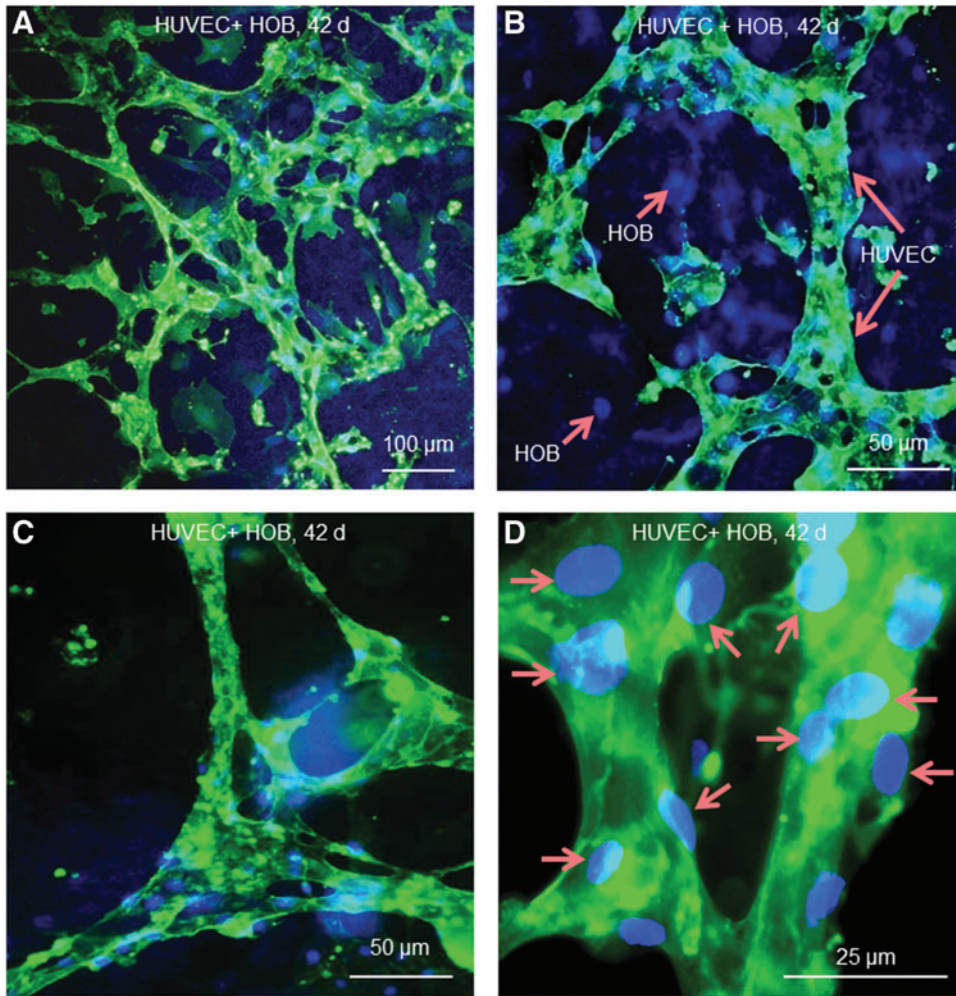


FIG. 2. Immunostaining of endothelial-specific PECAM1 on CPC with HUVEC+HOB coculture at 42 days. HUVEC and HOB were stained green. Both HUVEC and HOB nuclei were stained blue; however, the HOB had blue nuclei with no green staining. **(A)** HUVEC on macroporous CPC had self-assembled into a microcapillary-like structure with an extensive net-like pattern. **(B)** Higher magnification showed that the microcapillary-like structures (long arrows) extended throughout the HOB (short arrows). **(C)** The microcapillary-like structure was highly branched and interconnected. **(D)** Higher magnification revealed that the diameter of the microcapillary-like tubes consisted of two to three HUVEC, as indicated by the location of nuclei (arrows) and the PECAM1 staining. Color images available online at www.liebertpub.com/tea

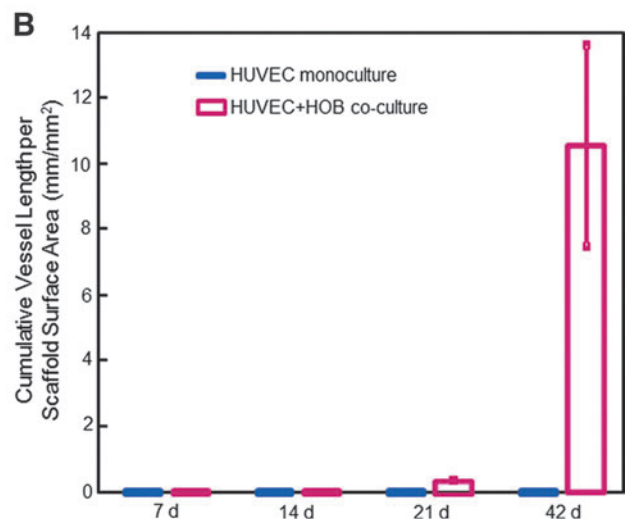
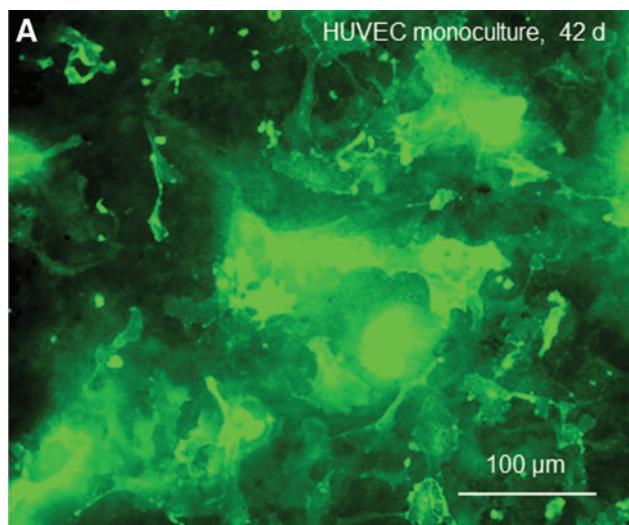


FIG. 3. **(A)** HUVEC monoculture on CPC at 42 days was immunostained for PECAM1. HUVEC attached well to macroporous CPC and proliferated and increased the coverage on the CPC surface. HUVEC distributed randomly as clumps or monolayers of cells, with no microcapillary-like structures on CPC. **(B)** Comparison of monoculture with coculture on macroporous CPC for microcapillary-like structure formation. The cumulative length of microcapillaries in each image was measured and divided by the area of the image (mean \pm SD; $n=6$). Color images available online at www.liebertpub.com/tea

FIG. 4. Immunohistochemical staining of thin sections of CPC construct after 42 days of HUVEC + HOB coculture. In (A), PECAM1 was stained into a brown/red color. Arrows indicate tube-like structures. PECAM1 staining confirmed the endothelial nature of the lumen-forming cells. In (B), the von Willebrand factor (vWF) was stained into a brown/red color. Arrows indicate microcapillary-like structures and lumens. In (C), collagen I was stained into a brown/red color. In (D), osteonectin (ON) was stained into a brown/red color. The pattern of ON staining appeared as clumps without a microcapillary-like structure, because ON is related to osteogenic differentiation and mineralization. Color images available online at www.liebertpub.com/tea

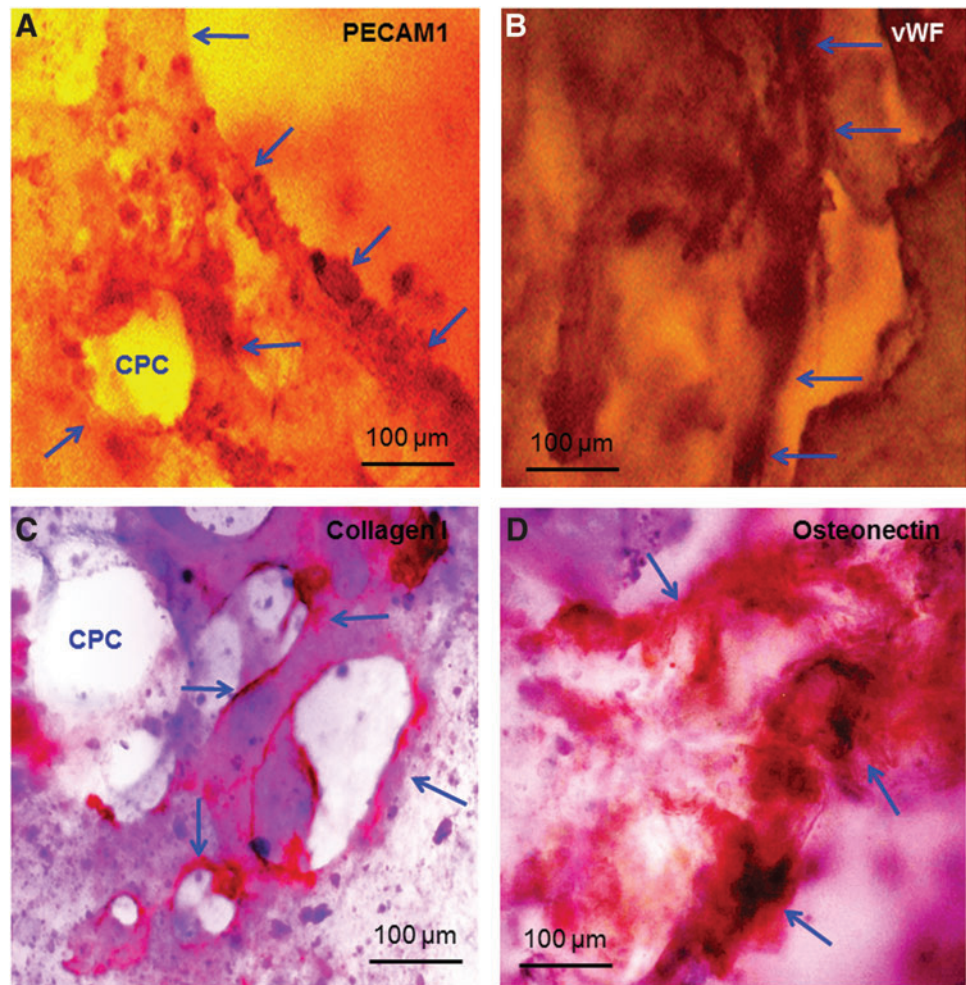


Figure 3B plots the cumulative vessel length (in unit mm) per CPC scaffold surface area (mm^2) (mean \pm SD; $n=6$). Monoculture produced no capillary-like structures on macroporous CPC from 7 to 42 days. Coculture of HUVEC + HOB on macroporous CPC started to form capillary-like structures at 21 days, which greatly increased at 42 days ($p < 0.05$).

In Figure 4, the growth of microcapillary-like structures (Fig. 4A–C) and osteogenesis (Fig. 4D) were determined by immunohistochemical staining of endothelial and osteoblast cell markers. At 42 days of coculture, microcapillary-like structures were strongly positive for PECAM1, which stained a brown/red color in Figure 4A. vWF was also stained a brown/red color in Figure 4B. Arrows in Figure 4A and B indicate tube-like structures and lumens. PECAM1 staining proved the endothelial nature of the lumen-forming cells. Collagen I staining was highly positive, showing as a brown/red color in Figure 4C. In Figure 4D, ON stained a brown/red color and was observed to spread throughout the CPC (arrows).

To further confirm the microcapillary-like structures, specimens were examined via SEM. Figure 5 shows representative images of vessel-like structures on CPC after 42 days of coculture. The morphology of microcapillary-like structures did not appear to be determined by the macropore

structures of CPC. For example, Figure 5A shows a microcapillary-like structure formed on the CPC surface where there were no macropores. In Figure 5B, the microcapillary appeared to form around the macropore edge in CPC, but then it deviated away from the edge of the macropore, indicated by the left arrow in Figure 5B. Therefore, these tube-like features appeared to be microcapillaries, and not merely cells aligning themselves along the edges of a macropore and reproducing the shape of a macropore. In addition, mineralization deposits were frequently observed, which were mingled and interconnected with the microcapillary structures on CPC.

Mineralization by the cells was further examined via ARS staining (Fig. 6). In Figure 6A, the CPC disk with no cell seeding showed a red color in ARS staining, because CPC consisted of apatite minerals. However, for CPC with cell seeding in coculture, the ARS staining became much thicker, producing a darker and denser red color, shown in Figure 6B and C at 21 and 42 days, respectively. These observations indicated a dense bone matrix formation on the construct. There was a layer of new mineralized matrix synthesized by the cells covering the CPC. The thick bone matrix covered not only the top surface, but also the peripheral areas at the sides of the construct. In Figure 6D, the cell-synthesized mineral amount (mean \pm SD; $n=6$) increased with time in

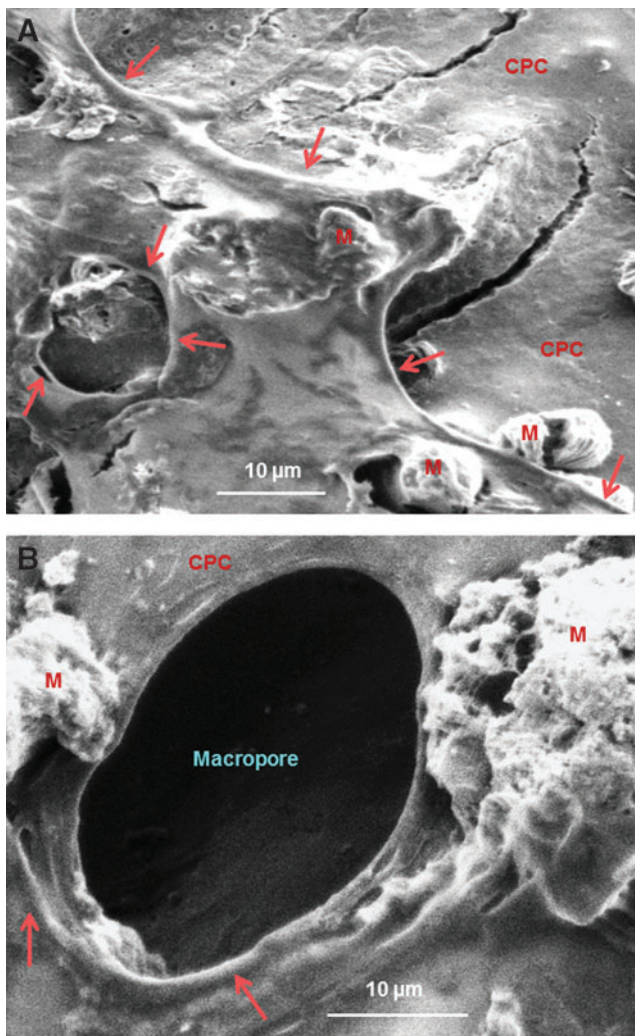


FIG. 5. Typical scanning electron microscopy images of microcapillary-like structures on CPC after 42 days of HUVEC + HOB coculture. CPC, macroporous calcium phosphate cement scaffold; M, mineral nodules synthesized by cells. In (A), a microcapillary-like structure formed on the CPC surface where there were no macropores. In (B), the microcapillary formed around the macropore edge in CPC, but then it deviated away from the edge of the macropore (left arrow in B). These observations suggest that the microcapillary-like structures were neovessels; they were not merely cells aligning themselves along the edges of a macropore to reproduce the shape of a macropore. Color images available online at www.liebertpub.com/tea

coculture on CPC ($p < 0.05$). These results indicate that the construct in coculture successfully underwent osteogenic differentiation and mineralization.

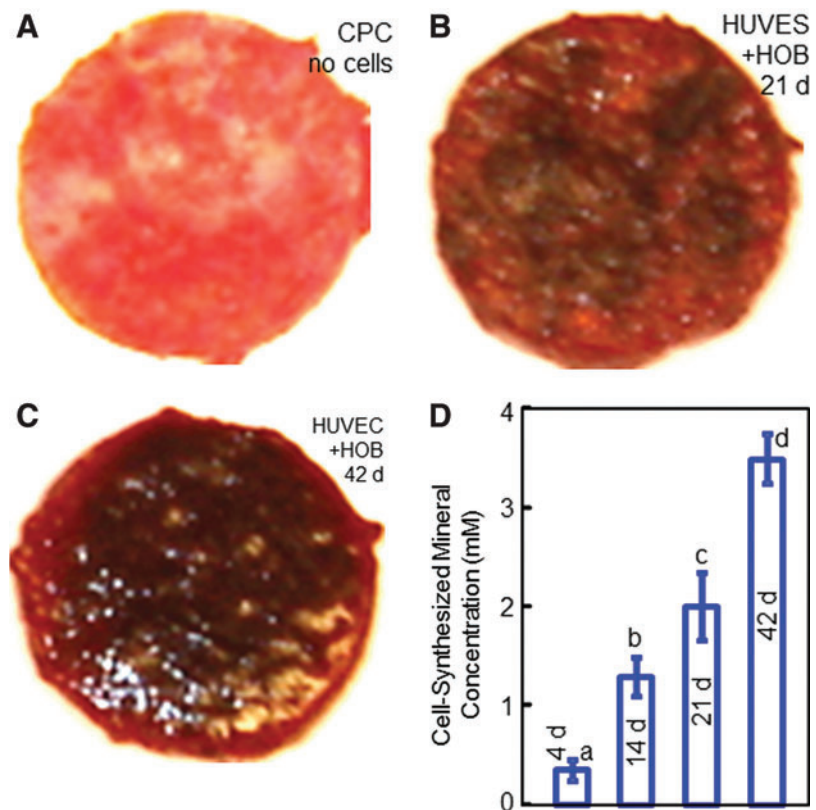
Discussion

The present study formulated an injectable, load-bearing, and macroporous CPC scaffold, investigated prevascularization via cell coculture *in vitro*, and formed microcapillary-like structures on CPC for the first time. The development of suitable scaffolds will constitute a centerpiece for bone tissue engineering. The structure needs to be

maintained to define the shape of the regenerated tissue. Mechanical properties are of crucial importance for the regeneration of load-bearing tissues such as bone, to withstand stresses to avoid scaffold fracture and to maintain the spaces in the scaffold for cell growth and tissue production.⁴⁵ In previous studies, hydrogels and other injectable polymers were developed for cell delivery and tissue engineering.^{46–50} Hydrogels were reported to have a strength of ~ 0.07 MPa and an elastic modulus of 0.1 MPa.^{46,49} Injectable polymeric carriers such as poly(propylene fumarate) were also developed for tissue engineering.⁴⁷ An injectable polymeric scaffold had a strength of 0.7 MPa and a modulus of 8 MPa.⁵⁰ In comparison, natural cancellous bone had a strength of ~ 3.5 MPa and a modulus of 300 MPa,^{51,52} much higher than those of injectable polymeric and hydrogel scaffolds. It was concluded that “Hydrogel scaffolds are used in non-load bearing bone tissue engineering....They do not possess the mechanical strength to be used in load bearing applications.”⁴⁸ In the present study, the CPC scaffold strength of 2.6 MPa and the elastic modulus of 340 MPa approached those of cancellous bone. The results of the present study showed that the mechanically strong and macroporous CPC scaffold was promising for *in vitro* prevascularization to enhance bone regeneration.

Prevacularization of tissue-engineering constructs is important for forming a microcapillary network to enhance implant performance. One approach is to obtain a prevascularized tissue-engineered scaffold *in vivo*.¹⁶ In this approach, the scaffold is first implanted in the recipient in a region with an abundant vascular supply, such as in a muscle site, for several weeks. This process results in the formation of a microvascular network in the construct. This construct with the microvascular network is then harvested and implanted at the bone defect site.¹⁶ The drawback of this approach is that it requires two surgeries with donor-site morbidity. Another approach is to obtain a prevascularized scaffold *in vitro*, and then implant it into the bone defect.^{17,19,20} Using this approach, a previous study cocultured endothelial cells in combination with osteoprogenitor cells, and demonstrated the *in vitro* formation of a three-dimensional prevascular network.¹⁹ In addition, the combination of endothelial cells with hMSCs likely enhanced the osteogenic differentiation of the hMSCs, manifested by the upregulation of ALP expression.¹⁹ Another study cocultured endothelial cells with HOB on fiber meshes, and formed microvessel-like structures *in vitro*.⁵³ Upon implantation *in vivo*, the endothelial cell-derived blood vessels were successfully integrated into the host tissue and anastomosed to the vascular supply.⁵³ In addition, a long-term coculture model was investigated that enhanced the *in vitro* vasculogenesis of HUVEC via coculture with HOB seeded in the polyurethane scaffold.⁴¹ The endothelial cell/osteoblast coculture was demonstrated to be an effective strategy for the *in vitro* formation of microcapillary-like structures containing a lumen, with the evolution from cord-like configuration to a branched morphology over time.²¹ In another study, a poly-3-caprolactone-hydroxyapatite scaffold was seeded with endothelial cells and osteoblasts, which yielded microvascular networks and the formation of bony matrix in grafts, and the resulting vascularization was able to promote osteogenesis in rats *in vivo*.⁵⁴ A literature search revealed few reports on the *in vitro* prevascularization of sintered CaP scaffolds.^{20,54} No report was found on *in vitro*

FIG. 6. Alizarin Red S staining of cell mineralization on CPC constructs. In (A), the CPC disk without cells was stained red, because CPC consisted of apatite minerals. In (B), the staining became thicker and darker on CPC with HUVEC+HOB coculture at 21 days. In (C), the staining became denser and appeared to be thicker at 42 days of coculture. The CPC was covered by a layer of new mineralized matrix synthesized by the cells. The new bone matrix covered not only the top surface, but also the peripheral areas at the sides of the construct. The results from the osteogenesis assay are plotted in (D). The cell-synthesized mineral amount greatly increased with coculture time on the CPC scaffold (mean \pm SD; $n=6$). Color images available online at www.liebertpub.com/tea



prevascularization of self-setting CPC. Therefore, the uniqueness of the present study is that the coculture method was shown to form a prevascularization network on a load-bearing and macroporous CPC for the first time.

HUVEC monoculture on macroporous CPC attached and proliferated, but exhibited little upregulation of angiogenic gene expression, and formed no microcapillary-like structure up to 42 days. In sharp contrast, the *VEGF* and collagen I expressions were highly upregulated in HUVEC+HOB coculture on CPC. The *VEGF* expression at 14 days was sixfold that at 1 day. This is consistent with an increase of about eightfolds for *VEGF* in a previous study.²¹ The time of peaking in these gene expressions was also similar to those observed previously. The present study observed that *VEGF* was minimal at 1 day, and then substantially increased at 14 and 21 days. These results are consistent with a previous study which showed that the *VEGF* was minimal at 7 days, and greatly increased at 14 and 21 days.²¹ In addition, the present study observed that the *ALP*, *OC*, and *Runx2* peaked at 14 and 21 days, consistent with previous studies.^{43,55} A study showed that the *ALP* was minimal at 1 day, and greatly increased at 14 and 21 days.⁵⁵ Another study reported that *OC* and collagen I peaked at 21 days, and *Runx2* peaked at 14 days.⁴³ PECAM1 staining and immunohistochemical staining on macroporous CPC identified elongated tube-like structures and multiple branches and sprouts in the present study. These microcapillary-like structures are also similar to those observed in previous studies.^{20,21} The diameter of the microcapillary consisted of two to three cells in the present study, also similar to previous findings.²⁰ The lumens were mingled with and extended through osteoblasts, consistent with previous observations.²⁰ Furthermore,

this observation was corroborated by SEM examination showing that the microcapillaries were interconnected with bone mineral nodules (Fig. 5).

The evidence that microcapillary-like structures were formed on macroporous CPC can be summarized in the following. First, high angiogenic gene expressions were obtained in coculture on CPC. Second, PECAM1 staining showed microcapillary-like structures with highly interconnected branches. PECAM1 is a cell-cell adhesion molecule, enabling cell-cell contacts, which are homotypic contacts. Homotypic contacts are important for the formation and maintenance of vessels.^{21,56} The endothelial cells on macroporous CPC migrated in self-assembly to organize into microcapillary-like structures. The existence of multiple sprouts and tube-like structures indicates that the lumens were branched and interconnected, and the prevascular network on macroporous CPC was highly interconnected, similar to those reported previously.^{20,21} Third, immunohistochemical staining of thin sections of CPC for PECAM1, vWF, and collagen I also showed extensive microvascular-like networks. Fourth, SEM examination revealed microcapillary-like structures on CPC, which did not follow macropore structures and were not due to the cells simply lining the pre-existing porous structures of CPC.

HUVEC+HOB coculture proved to be the key to prevascularizing the macroporous CPC scaffold, as HUVEC monoculture failed to form microcapillaries. Previous studies indicated a reciprocal regulation and functional relationship between endothelial cells and osteoblasts during osteogenesis.^{21,57} Endothelial cells affect the proliferation and differentiation of osteoblasts through soluble factors expressed by endothelial cells such as endothelin-1.⁵⁸ On the other hand,

osteoblasts can release antiogenic factors such as VEGF and bFGF to regulate the activity of endothelial cells.⁵⁹ Besides diffusible factors, endothelial cells and osteoblasts in coculture can also communicate via cell–cell contact mediated by proteins at gap junctions.^{20,60,61} These cellular interactions enabled the HUVEC+HOB coculture to successfully form microcapillary-like structures as well as bone minerals on the macroporous CPC scaffold.

Besides the importance of coculture, the properties of the scaffold also play an important role in prevascularization. Nanocrystalline hydroxyapatite was shown to stimulate angiogenesis.⁶² Hydroxyapatite was shown to absorb several important extracellular matrix proteins.^{63,64} Several CaP biomaterials, including hydroxyapatite were demonstrated to be osteoinductive, manifested by their ability to induce new bone formation in nonosseous sites such as in the muscles of large animals, without the delivery of cells or growth factors.^{65,66} This osteoinduction did not appear to be closely related to the chemistry of the materials.^{30,66} Instead, the physical morphology of the biomaterial, including its macroporous structure and microporous surface appeared to be critical to osteoinduction and ectopic bone formation.^{30,66} It was postulated that osteoinductive biomaterials such as hydroxyapatite could adsorb endogenous growth factors from the body fluids *in vivo*, which in turn would facilitate the relevant pluripotent stem cells to form new bone.⁶⁷ The CPC of the present study could self-harden to form nanocrystalline hydroxyapatite with a highly porous structure, which could be suitable to stimulate angiogenesis and bone regeneration. The *in vitro* prevascularization of the macroporous CPC, coupled with its good mechanical properties, may enable the prevascularized CPC construct to greatly facilitate and improve bone regeneration. It should be noted that the prevascularized CPC in the present pilot study is a preformed construct and not injectable. Once the benefits of codelivering osteogenic cells and endothelial cells with CPC are established, it is possible to encapsulate both cells in degradable hydrogel microbeads in the CPC paste, which can be injected without harming the cells.^{38,43} This injectable CPC-cell paste would then harden in the bone defect to form a macroporous scaffold to improve bone regeneration and vascularization. In addition, resorbable fibers could be included in the injectable paste for mechanical reinforcement.³⁸ Potential applications include various orthopedic repairs and dental and craniofacial regenerations.^{38,55} Further studies are needed to investigate the codelivery of osteogenic cells and endothelial cells via CPC in animal models.

Conclusions

A gas-foaming macroporous CPC scaffold was fabricated and HUVEC+HOB coculture was performed for prevascularization, yielding microcapillary-like structures on the CPC scaffold for the first time. The formation of microcapillary-like structures was evidenced by highly elevated angiogenic expressions of VEGF and collagen I, histological analyses, and SEM examinations. The formation of extensive self-assembled vascular-like networks on CPC was achieved in coculture, but not in monoculture. PECAM1, collagen I, and vWF immunohistochemical assays and SEM examination revealed highly interconnected vascular-like structures on CPC. The cumulative vessel length per scaffold surface

area greatly increased in coculture up to 42 days. HOB in coculture showed excellent differentiation with elevated ALP, OC, and *Runx2* expressions, with synthesis of a mineralized bone matrix on CPC. The cell-synthesized mineral concentration increased by an order of magnitude from 4 to 42 days. These findings indicate the feasibility of generating a prevascularized network on macroporous CPC before implantation *in vivo* to enhance bone regeneration and tissue function. The novel macroporous CPC-microvasculature construct is promising for orthopedic and craniofacial applications.

Acknowledgments

We gratefully thank Dr. Michael D. Weir for experimental help and discussions in making the immunohistochemical analysis. We also thank Dr. L.C. Chow of the Paffenbarger Research Center and Dr. Carl G. Simon at the National Institute of Standards and Technology for fruitful discussions. This study was supported by NIH R01 DE14190 and R21 DE22625 (HX) and the University of Maryland School of Dentistry.

Disclosure Statement

No competing financial interests exist.

References

1. Praemer, A., Furner, S., and Rice, D.P. Musculoskeletal Conditions in the United States. Rosemont: American Academy of Orthopaedic Surgeons, 1999.
2. United States Bone and Joint Decade (USBJD) 2002–2011. The Burden of Musculoskeletal Diseases in the United States. Rosemont, IL: American Academy of Orthopaedic Surgeons, 2008, Foreword.
3. Mikos, A.G., Herring, S.W., Ochareon, P., Elisseeff, J., Lu, H.H., Kandel, R., Schoen, F.J., Toner, M., Mooney, D., Atala, A., Van Dyke, M.E., Kaplan, D., and Vunjak-Novakovic, G. Engineering complex tissues. *Tissue Eng* **12**, 3307, 2006.
4. Ginebra, M.P., Traykova, T., and Planell, J.A. Calcium phosphate cements as bone drug-delivery systems: a review. *J Controlled Release* **113**, 102, 2006.
5. Russias, J., Saiz, E., Deville, S., Gryn, K., Liu, G., and Tomsia, A.P. Fabrication and *in vitro* characterization of three-dimensional organic/inorganic scaffolds by robocasting. *J Biomed Mater Res A* **83**, 434, 2007.
6. Mao, J.J., Vunjak-Novakovic, G., Mikos, A.G., and Atala, A. *Regenerative Medicine: Translational Approaches and Tissue Engineering*. Boston, MA: Artech House, 2007.
7. Bohner, M. Design of ceramic-based cements and putties for bone graft substitution. *Eur Cell Mater* **20**, 1, 2010.
8. Leach, J.K., Kaigler, D., Wang, Z., Krebsbach, P.H., and Mooney, D.J. Coating of VEGF-releasing scaffolds with bioactive glass for angiogenesis and bone regeneration. *Biomaterials* **27**, 3249, 2006.
9. Mao, J.J., Giannobile, W.V., Helms, J.A., Hollister, S.J., Krebsbach, P.H., Longaker, M.T., and Shi, S. Craniofacial tissue engineering by stem cells. *J Dent Res* **85**, 966, 2006.
10. Johnson, P.C., Mikos, A.G., Fisher, J.P., and Jansen, J.A. Strategic directions in tissue engineering. *Tissue Eng* **13**, 2827, 2007.
11. Radin, S., Reilly, G., Bhargava, G., Leboy, P.S., and Ducheyne, P. Osteogenic effects of bioactive glass on bone marrow stromal cells. *J Biomed Mater Res A* **73**, 21, 2005.

12. Jansen, J.A., Vehof, J.W.M., Ruhe, P.Q., Kroeze-Deutman, H., Kuboki, Y., Takita, H., Hedberg, E.L., and Mikos, A.G. Growth factor-loaded scaffolds for bone engineering. *J Controlled Release* **101**, 127, 2005.
13. Benoit, D.S.W., Nuttelman, C.R., Collins, S.D., and Anseth, K.S. Synthesis and characterization of a fluvastatin-releasing hydrogel delivery system to modulate hMSC differentiation and function for bone regeneration. *Biomaterials* **27**, 6102, 2006.
14. Morgan, A.W., Roskov, K.E., Lin-Gibson, S., Kaplan, D.L., Becker, M.L., and Simon, Jr., C.G. Characterization and optimization of RGD-containing silk blends to support osteoblastic differentiation. *Biomaterials* **29**, 2556, 2008.
15. Chen, W., Zhou, H., Weir, M.D., Bao, C., and Xu, H.H.K. Umbilical cord stem cells released from alginate-fibrin microbeads inside macroporous and biofunctionalized calcium phosphate cement for bone regeneration. *Acta Biomater* **8**, 2297, 2012.
16. Rouwkema, J., Rivron, N.C., and van Blitterswijk, C.A. Vascularization in tissue engineering. *Trends Biotech* **26**, 434, 2008.
17. Lovett, M., Lee, K., Edwards, A., and Kaplan, D.L. Vascularization strategies for tissue engineering. *Tissue Eng Part B* **15**, 353, 2009.
18. Barralet, J., Gbureck, U., Habibovic, P., Vorndran, E., Gerard, C., and Doillon, C.J. Angiogenesis in calcium phosphate scaffolds by inorganic copper ion release. *Tissue Eng A* **15**, 1601, 2009.
19. Rouwkema, J., De Boer, J., and van Blitterswijk, C.A. Endothelial cells assemble into a 3-dimensional prevascular network in a bone tissue engineering construct. *Tissue Eng* **12**, 2685, 2006.
20. Unger, R.E., Sartoris, A., Peters, K., Motta, A., Migliaresi, C., Kunkel, M., Bulnheim, U., Rychly, J., and Kirkpatrick, C.J. Tissue-like self-assembly in cocultures of endothelial cells and osteoblasts and the formation of microcapillary-like structures on three-dimensional porous biomaterials. *Biomaterials* **28**, 3965, 2007.
21. Santos, M.I., Unger, R.E., Sousa, R.A., Reis, R.L., and Kirkpatrick, C.J. Crosstalk between osteoblasts and endothelial cells co-cultured on a polycaprolactone-starch scaffold and the *in vitro* development of vascularization. *Biomaterials* **30**, 4407, 2009.
22. Chow, L.C. Calcium phosphate cements: chemistry, properties, and applications. *Mat Res Symp Proc* **599**, 27, 2000.
23. Barralet, J.E., Gaunt, T., Wright, A.J., Gibson, I.R., and Knowles, J.C. Effect of porosity reduction by compaction on compressive strength and microstructure of calcium phosphate cement. *J Biomed Mater Res B* **63**, 1, 2002.
24. Ruhe, P.Q., Hedberg, E.L., Padron, N.T., Spauwen, P.H., Jansen, J.A., and Mikos, A.G. rhBMP-2 release from injectable poly(DL-lactic-co-glycolic acid)/calcium-phosphate cement composites. *J Bone Joint Surg Am* **85-A Suppl 3**, 75, 2003.
25. Simon, C.G., Guthrie, W.F., and Wang, F.W. Cell seeding into calcium phosphate cement. *J Biomed Mater Res A* **68**, 628, 2004.
26. Xu, H.H.K., and Simon, C.G. Fast setting calcium phosphate-chitosan scaffold: mechanical properties and biocompatibility. *Biomaterials* **26**, 1337, 2005.
27. Deville, S., Saiz, E., Nalla, R.K., and Tomsia, A.P. Freezing as a path to build complex composites. *Science* **311**, 515, 2006.
28. Bodde, E.W., Boerman, O.C., Russel, F.G., Mikos, A.G., Spauwen, P.H., and Jansen, J.A. The kinetic and biological activity of different loaded rhBMP-2 calcium phosphate cement implants in rats. *J Biomed Mater Res A* **87**, 780, 2008.
29. Bohner, M., and Baroud, G. Injectability of calcium phosphate pastes. *Biomaterials* **26**, 1553, 2005.
30. Habibovic, P., Gbureck, U., Doillon, C.J., Bassett, D.C., van Blitterswijk, C.A., and Barralet, J.E. Osteoconduction and osteoinduction of low-temperature 3D printed bioceramic implants. *Biomaterials* **29**, 944, 2008.
31. Friedman, C.D., Costantino, P.D., Takagi, S., and Chow, L.C. BoneSource hydroxyapatite cement: a novel biomaterial for craniofacial skeletal tissue engineering and reconstruction. *J Biomed Mater Res* **43**, 428, 1998.
32. Ginebra, M.P., Driessens, F.C., and Planell, J.A. Effect of the particle size on the micro and nanostructural features of a calcium phosphate cement: a kinetic analysis. *Biomaterials* **25**, 3453, 2004.
33. Ruhe, P.Q., Hedberg-Dirk, E.L., Padron, N.T., Spauwen, P.H., Jansen, J.A., and Mikos, A.G. Porous poly(DL-lactic-co-glycolic acid)/calcium phosphate cement composite for reconstruction of bone defects. *Tissue Eng* **12**, 789, 2006.
34. Bodde, E.W., Habraken, J.E., Mikos, A.G., Spauwen, P.H., and Jansen, J.A. Effect of polymer molecular weight on the bone biological activity of biodegradable polymer/calcium phosphate cement composites. *Tissue Eng A* **15**, 3183, 2009.
35. Xu, H.H.K., and Quinn, J.B. Calcium phosphate cement containing resorbable fibers for short-term reinforcement and macroporosity. *Biomaterials* **23**, 193, 2002.
36. Xu, H.H.K., Takagi, S., Quinn, J.B., and Chow, L.C. Fast-setting and anti-washout calcium phosphate scaffolds with high strength and controlled macropore formation rates. *J Biomed Mater Res A* **68**, 725, 2004.
37. Burguera, E.F., Xu, H.H.K., and Weir, M.D. Injectable and rapid-setting calcium phosphate bone cement with dicalcium phosphate dihydrate. *J Biomed Mater Res B* **77**, 126, 2006.
38. Zhao, L., Weir, M.D., and Xu, H.H.K. An injectable calcium phosphate - alginate hydrogel - umbilical cord mesenchymal stem cell paste for bone tissue engineering. *Biomaterials* **31**, 6502, 2010.
39. Chen, W., Zhou, H., Tang, M., Weir, M.D., Bao, C., and Xu, H.H.K. Gas-foaming calcium phosphate cement scaffold encapsulating human umbilical cord stem cells. *Tissue Eng A* **18**, 816, 2012.
40. Xu, H.H.K., Quinn, J.B., Takagi, S., Chow, L.C., and Eichmiller, F.C. Strong and macroporous calcium phosphate cement: effects of porosity and fiber reinforcement on mechanical properties. *J Biomed Mater Res* **57**, 457, 2001.
41. Hofmann, A., Ritz, U., Verrier, S., Eglin, D., Alini, M., Fuchs, S., Kirkpatrick, C.J., and Rommens, P.M. The effect of human osteoblasts on proliferation and neo-vessel formation of human umbilical vein endothelial cells in a long-term 3D coculture on polyurethane scaffolds. *Biomaterials* **29**, 4217, 2008.
42. Livak, K.J., and Schmittgen, T.D. Analysis of relative gene expression data using real-time quantitative PCR and the $2^{-\Delta\Delta Ct}$ Method. *Methods* **25**, 402, 2001.
43. Zhou, H., and Xu, H.H.K. The fast release of stem cells from alginate-fibrin microbeads in injectable scaffolds for bone tissue engineering. *Biomaterials* **32**, 7503, 2011.
44. Thein-Han, W.W., and Xu, H.H.K. Collagen-calcium phosphate cement scaffolds seeded with umbilical cord stem cells for bone tissue engineering. *Tissue Eng A* **17**, 2943, 2011.
45. Chaikof, E.L., Matthew, H., Kohn, J., Mikos, A.G., Prestwich, G.D., and Yip, C.M. Biomaterials and scaffolds in reparative medicine. *Ann NY Acad Sci* **961**, 96, 2002.

46. Kuo, C.K., and Ma, P.X. Ionically crosslinked alginate hydrogels as scaffolds for tissue engineering: Part I. Structure, gelation rate and mechanical properties. *Biomaterials* **22**, 511, 2001.
47. Payne, R.G., Yaszemski, M.J., Yasko, A.W., and Mikos, A.G. Development of an injectable, *in situ* crosslinkable, degradable polymeric carrier for osteogenic cell populations. Part 1. Encapsulation of marrow stromal osteoblasts in surface crosslinked gelatin microparticles. *Biomaterials* **23**, 4359, 2002.
48. Drury, J.L., and Mooney, D.J. Review. Hydrogels for tissue engineering: scaffold design variables and applications. *Biomaterials* **24**, 4337, 2003.
49. Drury, J.L., Dennis, R.G., and Mooney, D.J. The tensile properties of alginate hydrogels. *Biomaterials* **25**, 3187, 2004.
50. Shi, X., Sitharaman, B., Pham, Q.P., Liang, F., Wu, K., Billups, W.E., Wilson, L.J., and Mikos, A.G. Fabrication of porous ultrashort single-walled carbon nanotube nanocomposite scaffolds for bone tissue engineering. *Biomaterials* **28**, 4078, 2007.
51. O'Kelly, K., Tancred, D., McCormack, B., and Carr, A. A quantitative technique for comparing synthetic porous hydroxyapatite structure and cancellous bone. *J Mater Sci Mater Med* **7**, 207, 1996.
52. Broz, J.J., Simske, S.J., Corley, W.D., and Greenberg, A.R. Effects of deproteinization and ashing on site-specific properties of cortical bone. *J Mater Sci Mater Med* **8**, 395, 1997.
53. Fuchs, S., Ghanaati, S., Orth, C., Barbeck, M., Kolbe, M., Hofmann, A., Eblenkamp, M., Gomes, M., Reis, R.L., and Kirkpatrick, C.J. Contribution of outgrowth endothelial cells from human peripheral blood *in vivo* vascularization of bone tissue engineered constructs based on starch polycaprolactone scaffolds. *Biomaterials* **30**, 526, 2009.
54. Yu, H., VandeVord, P.J., Mao, L., Matthew, H.W., Wooley, P.H., and Yang, S.Y. Improved tissue-engineered bone regeneration by endothelial cell mediated vascularization. *Biomaterials* **30**, 508, 2009.
55. Xu, H.H.K., Zhao, L., and Weir, M.D. Stem cell-calcium phosphate constructs for bone engineering. *J Dent Res* **89**, 1482, 2010.
56. Simon, A.M., and McWhorter, A.R. Vascular abnormalities in mice lacking the endothelial gap junction proteins connexin37 and connexin40. *Dev Biol* **251**, 206, 2002.
57. Villars, F., Bordenave, L., Bareille, R., and Amedee, J. Effect of human endothelial cells on human bone marrow stromal cell phenotype: role of VEGF? *J Cell Biochem* **79**, 672, 2000.
58. Kasperk, C.H., Borcsok, I., Schairer, H.U., Schneider, U., Nawroth, P.P., Niethard, F.U., and Ziegler, R. Endothelin-1 is a potent regulator of human bone cell metabolism *in vitro*. *Calcif Tissue Int* **60**, 368, 1997.
59. Deckers, M.M.L., van Bezooijen, R.L., van der Horst, G., Hoogendam, J., van der Bent, C., Papapoulos, S.E., and Löwik, C.W. Bone morphogenetic proteins stimulate angiogenesis through osteoblast-derived vascular endothelial growth factor A. *Endocrinology* **143**, 1545, 2002.
60. Villars, F., Guillotin, B., Amedee, T., Dutoya, S., Bordenave, L., Bareille, R., and Amédée, J. Effect of HUVEC on human osteoprogenitor cell differentiation needs heterotypic gap junction communication. *Am J Physiol Cell Physiol* **282**, C775, 2002.
61. Wenger, A., Stahl, A., Weber, H., Finkenzeller, G., Augustin, H.G., Stark, G.B., and Kneser, U. Modulation of *in vitro* angiogenesis in a three-dimensional spheroidal coculture model for bone tissue engineering. *Tissue Eng* **10**, 1536, 2004.
62. Kilian, O., Fuhrmann, R., Alt, V., Noll, T., Coskun, S., Dingeldein, E., Schnettler, R., and Franke, R.P. Plasma transglutaminase factor XIII induces microvessel ingrowth into biodegradable hydroxyapatite implants in rats. *Biomaterials* **26**, 1819, 2005.
63. Stayton, P.S., Drobny, G.P., Shaw, W.J., Long, J.R., and Gilbert, M. Molecular recognition at the protein-hydroxyapatite interface. *Crit Rev Oral Biol Med* **14**, 370, 2003.
64. Pezzatini, S., Solito, R., Morbidelli, L., Lamponi, S., Boanini, E., Bigi, A., and Ziche, M. The effect of hydroxyapatite nanocrystals on microvascular endothelial cell viability and functions. *J Biomed Mater Res A* **76**, 656, 2006.
65. Ripamonti, U. Osteoinduction in porous hydroxyapatite implanted in heterotopic sites of different animal models. *Biomaterials* **17**, 31, 1996.
66. Yuan, H., Fernandes, H., Habibovic, P., de Boer, J., Barradas, A.M., de Ruiter, A., Walsh, W.R., van Blitterswijk, C.A., and de Bruijn, J.D. Osteoinductive ceramics as a synthetic alternative to autologous bone grafting. *Proc Natl Acad Sci U S A* **107**, 13614, 2010.
67. De Groot, J. Carriers that concentrate native bone morphogenetic protein *in vivo*. *Tissue Eng* **4**, 337, 1998.

Address correspondence to:

Hockin H.K. Xu, PhD

Biomaterials & Tissue Engineering Division
Department of Endodontics, Prosthodontics and
Operative Dentistry
University of Maryland Dental School
650 West Baltimore St.
Baltimore, MD 21201

E-mail: hxu@umaryland.edu

Received: October 24, 2012

Accepted: February 18, 2013

Online Publication Date: April 16, 2013